

Article

# Preparation and Characterization of Polystyrene Hybrid Composites Reinforced with 2D and 3D Inorganic Fillers

Athanasios Ladavos <sup>1,\*</sup>, Aris E. Giannakas <sup>2</sup>, Panagiotis Xidas <sup>3</sup>, Dimitrios J. Giliopoulos <sup>3</sup>,  
Maria Baikousi <sup>4</sup>, Dimitrios Gournis <sup>4</sup>, Michael A. Karakassides <sup>4</sup> and Konstantinos S. Triantafyllidis <sup>3</sup>

<sup>1</sup> Laboratory of Food Technology, Department of Business Administration of Food and Agricultural Enterprises, University of Patras, 30100 Agrinio, Greece

<sup>2</sup> Department of Food Science and Technology, University of Patras, 30100 Agrinio, Greece; agiannakas@upatras.gr

<sup>3</sup> Department of Chemistry, Aristotle University of Thessaloniki, 54124 Thessaloniki, Greece; pxidas.mail@gmail.com (P.X.); dgiliopo@chem.auth.gr (D.J.G.); ktrianta@chem.auth.gr (K.S.T.)

<sup>4</sup> Department of Materials Science & Engineering, University of Ioannina, 45110 Ioannina, Greece; mbaikou@cc.uoi.gr (M.B.); dgourni@uoi.gr (D.G.); mkarakas@uoi.gr (M.A.K.)

\* Correspondence: alantavo@upatras.gr

**Abstract:** Polystyrene (PS)/silicate composites were prepared with the addition of two organoclays (orgMMT and orgZenith) and two mesoporous silicas (SBA-15 and MCF) via (i) solution casting and (ii) melt compounding methods. X-ray diffraction (XRD) analysis evidenced an intercalated structure for PS/organoclay nanocomposites. Thermogravimetric analysis indicated improvement in the thermal stability of PS-nanocomposites compared to the pristine polymer. This enhancement was more prevalent for the nanocomposites prepared with a lab-made organoclay (orgZenith). Tensile measurement results indicated that elastic modulus increment was more prevalent (up to 50%) for microcomposites prepared using mesoporous silicas as filler. Organoclay addition led to a decrease in oxygen transmission rate (OTR) values. This decrement reached up to 50% for high organoclay content films in comparison to pristine PS film. Decrement above 80% was measured for microcomposites with mesoporous silicas and 5 wt% filler content obtained via melt compounding.

**Keywords:** polystyrene; nanocomposites; microcomposites; organoclay; mesoporous silicas



**Citation:** Ladavos, A.; Giannakas, A.E.; Xidas, P.; Giliopoulos, D.J.; Baikousi, M.; Gournis, D.; Karakassides, M.A.; Triantafyllidis, K.S. Preparation and Characterization of Polystyrene Hybrid Composites Reinforced with 2D and 3D Inorganic Fillers. *Micro* **2021**, *1*, 3–14. <https://doi.org/10.3390/micro1010002>

Academic Editor: Eiichi Tamiya

Received: 1 April 2021

Accepted: 25 April 2021

Published: 7 May 2021

**Publisher's Note:** MDPI stays neutral with regard to jurisdictional claims in published maps and institutional affiliations.



**Copyright:** © 2021 by the authors. Licensee MDPI, Basel, Switzerland. This article is an open access article distributed under the terms and conditions of the Creative Commons Attribution (CC BY) license (<https://creativecommons.org/licenses/by/4.0/>).

## 1. Introduction

Different types of nano-reinforcement in combination with polymer find application in various areas of engineering and technology due to their exceptional properties, such as improved thermal stability, water and oxygen barrier, mechanical strength, flame retardancy, chemical resistance, optical, magnetic, and electrical properties [1–3]. For the development of polymer nanocomposites, various nanofillers have been used. These may be one-dimensional, which includes, fibers, cellulose whiskers, and carbon nanotubes [4,5], two-dimensional, which includes clays and graphene [6,7], and three-dimensional, which includes spherical particles like alumina, silica, titania, latex, metallic particles, etc. [8–10]. The use of a specific phase at the nanoscale aims at tailoring the properties of the system for specific applications.

Polymer nanocomposites are prepared by three main processes—in situ polymerization, melt compounding, and solution mixing. These three techniques may be used in combination with each other or individually to achieve the preferred structure of nanocomposites. Two characteristics of the nano-additive influence the nanocomposite's quality and must be taken into consideration: particle size and distribution. Small and well-distributed particles lead to the reinforcement of the nanocomposite's properties.

One of the most applied techniques is the use of polymer/clay nanocomposites (PCNs), since they have the capacity to generate new polymer properties. PCNs have the

capacity to generate improved polymer properties due to their ability to disperse particles of clay on a nanometer scale in the polymeric matrix. Incorporation of a small amount of nano-additives has been found to greatly improve polymer's properties, such as gas barrier, modulus, strength, chemical resistance, and flame retardancy. To achieve these properties, several factors must be considered: nature, type, properties, and structure of clay and clay modifiers. The most important factors are the size of clay particles and compatibility between the polymer matrix and clay [11–18].

Since many polymers are hydrophobic, a surfactant must be used to modify hydrophilic clay so the gallery space will be sufficiently hydrophobic to interact with the polymer. In a recent review, Panwar et al. [15] concluded that most of the PS/clay nanocomposites having exfoliated structures have been prepared by the in situ polymerization method. Melt compounding, on the other hand, seems to be a promising method due to its commercial applicability. Further, new procedures, such as modification of polymers or clay organic modification and the addition of compatibilizers, have resulted in successful formation of exfoliated structures. The solution mixing method has also been used for the preparation of PS nanocomposites. However, the use of solvent impedes its industrial applicability. PS nanocomposites prepared by various techniques have shown improved thermal and mechanical properties in addition to enhanced properties such as gas barrier and flame retardancy.

Apart from layered silicates, polymer nanocomposites with other inorganic nano-oxides, such as nano-silica ( $\text{SiO}_2$ ), nano-alumina ( $\text{Al}_2\text{O}_3$ ), titanium dioxide ( $\text{TiO}_2$ ), mesoporous MCM, layered double hydroxide, etc., have also been discussed [19–23]. Jeon et al. presented a review of recent progress in polymer-based inorganic nanoparticle composites. It was suggested that the mechanical properties of nanocomposites prepared from various polymers (PU, EP, PA6, polyimide (PI), PP, PET, polystyrene (PS)) and inorganic particles (layered silicates,  $\text{SiO}_2$ , zinc sulfide (ZnS),  $\text{TiO}_2$ ) did not always increase due to aggregation of the inorganic particles in the polymer matrices. It was suggested to optimize the content of the inorganic particles or to use organic additives as functionalized to avoid aggregation. Kango et al. [21] provided a review of the effect of surface modification of inorganic nanoparticles for the development of organic-inorganic nanocomposites. A series of matrices (PA6, PA6.6, acrylonitrile butadiene styrene (ABS), polyester, EP, polyphenylene sulfide (PPS), PMMA, polycarbonate (PC), etc.) in combination with inorganic particles ( $\text{SiO}_2$ , calcium carbonate ( $\text{CaCO}_3$ ),  $\text{Al}_2\text{O}_3$ ,  $\text{TiO}_2$ , silicon carbide (SiC), zinc oxide (ZnO), etc.) was reported in terms of their mechanical and tribological properties. The main conclusion drawn was that surface modification improved the interfacial interactions between the inorganic nanofillers and polymer matrices, which resulted in unique properties, such as very high mechanical toughness (even at low loadings of inorganic reinforcements). The effect of MCM-41 particles on the thermal properties of tailor-made polystyrene/MCM-41 nanocomposites via the in situ method was investigated [22]. A noticeable decrease in conversion and molecular weights and increase of polydispersity index from 1.14 to 1.41 were observed after a 3 wt% addition of MCM-41 nanoparticles in the polymerization media. Moreover, increasing of thermal stability and a decrease in glass-transition temperature ( $T_g$ ) values from 100.3 to 85.9 °C were two important results of 3 wt% addition of MCM-41 nanoparticles into the polystyrene matrix. In a previous report [23], the development of polystyrene nanocomposites through solvent blending technique with different contents of modified Co-Al layered double hydroxide (LDH) (1–7 wt%) was presented. The X-ray diffraction (XRD) results suggested the formation of exfoliated structure, while transmission electron microscopy (TEM) images clearly indicated the intercalated morphology of PS nanocomposites at higher loading.

In this paper, (i) solution mixing and (ii) melt compounding methods for composite preparation were applied to prepare a series of polystyrene nano- or micro-composite materials. Polystyrene (PS) is a thermoplastic widely used in various applications, such as packaging and household items, due to its low cost and transparency. The aim of this work was to study the influence of 2D organo-modified nano-clay and 3D mesoporous

inorganic microfillers, on tensile, thermal, and barrier properties of polystyrene hybrid materials prepared in the form of film. The additional goal was to determine the optimum filler type and content for the enhancement of the composite's properties.

## 2. Materials and Methods

### 2.1. Raw Materials—Organic Modification of Nanoclay

Polystyrene (PS) was obtained from Aldrich Chem. Company, Hamburg, Germany, with weight and number average molecular weights of  $M_w = 230,000$  g/mol and  $M_n = 140,000$  g/mol, respectively.

The layered silicates (clays) used in this work were (i) organo-montmorillonite (orgMMT) NANOMER<sup>®</sup>-I.44P, produced by Nanocor Company, Aberdeen, MS, USA and supplied by Aldrich. NANOMER<sup>®</sup>-I.44P is an onium ion-modified clay containing ~40 wt% dimethyl dialkyl (C14-18) ammonium surfactant. (ii) Lab-made organo-modified bentonite (brand Zenith, S&B Co, Athens, Greece) from the Greek island of Milos in the Aegean Sea. Lab-modified clay with code name orgZenith was obtained using the surfactant used by Nanocor in NANOMER<sup>®</sup>-I.44P organoclay, namely Arquad<sup>®</sup> 2HT-75, produced by Akzo and supplied by Fluka. To prepare organo-modified clay, a 1 wt% solution of surfactant in warm water was prepared and added dropwise to a 1 wt% clay suspension in the same solvent. The obtained mixture was stirred vigorously for 24 h at 70 °C. The amount of the surfactant added was equivalent to 1.5 times the cation exchange capacity (CEC) of clay. The resulting samples were washed four times with deionized water and once with ethanol in order to remove the excess of surfactant, and dried in a vacuum oven at 40 °C [14].

The SBA-15 and MCF mesoporous silicas used in this study were synthesized according to previous methodologies [24–26] via the cooperative self-assembly method, using tetraethyl orthosilicate (TEOS) as the silica source, Pluronic P123 as the structure directing agent, and, in the case of MCF, mesitylene as the “swelling agent” and  $\text{NH}_4\text{F}$  for the control of the pore window size. In a typical SBA-15 synthesis, Pluronic P123 was initially added in aqueous 1.6 M HCl and the mixture was stirred until the formation of a crystal-clear solution. The appropriate amount of TEOS was then added and the mixture was stirred for some additional time. Thereafter, the mixture was placed in a propylene autoclave and was thermally treated (aging). The hybrid silica was recovered via filtration, washed with deionized water, and dried in air. The resulting powder was calcined to produce the final mesoporous material. The MCF synthesis was identical to SBA-15, except for the use of mesitylene and  $\text{NH}_4\text{F}$  that were added to the mixture after the mixing with TEOS and before the step of thermal aging. The reactants' molar ratios for SBA-15 and MCF syntheses were: TEOS (1)/P123 (0.018)/HCl (3.33)/ $\text{H}_2\text{O}$  (97.5) and TEOS (1)/P123 (0.018)/TMB (0.87)/ $\text{NH}_4\text{F}$  (0.3)/HCl (3.33)/ $\text{H}_2\text{O}$  (97.5), respectively.

### 2.2. Preparation of PS/Composites

Polystyrene composites with 1, 3, and 5 wt% filler loadings of two organoclays and two mesoporous silicas were prepared via the solution casting method, as described previously [13]. An appropriate amount of PS was diluted in  $\text{CHCl}_3$  and the solution was mixed, under vigorous stirring, with the filler suspension in the same solvent. After 24 h of stirring, the mixtures were cast onto plastic dishes (14 cm diameter). The castings were dried at ambient conditions and then the plastic plates were peeled off. The as-received films were further pressed for 2 min at 160 °C under 2 ton constant pressure, using a hydraulic press with heated platens.

Moreover, PS/composites with 1, 3, and 5 wt% SBA-15 and MCF filler loadings (designated with the letter “m” in their code names) were prepared by melting, at 180 °C in an oven, appropriate amounts of PS and SBA-15 or MCF. For better homogenization, periodical mechanical stirring (out of the oven) using a micromixer (IKA- WERKE model DI 25) with a stirring speed of 8000 rpm was applied. Final films were received after hot-pressing for 2 min at 160 °C under 2 ton constant pressure, using a hydraulic press with heated platens.

### 2.3. Characterization

Scanning electron microscopy (SEM) images of SBA-15 and MCF mesoporous silicas were obtained with an electron microscope Zeiss Supra 55 VP, Jena, Germany. The accelerating voltage was 15.00 kV, and the scanning was performed on a sample powder. All the studied samples were coated with carbon black to avoid charging under the electron beam.

TEM experiments of SBA-15 and MCF mesoporous silicas were carried out on a JEOL 2011 TEM with a LaB<sub>6</sub> filament and an accelerating voltage of 200 kV. The specimens were prepared by evaporating drops of SBA-15 or MCF silica–ethanol suspension after sonication onto a carbon-coated lacy film supported on a 3 mm diameter, 300 mesh copper grid.

Nitrogen adsorption/desorption experiments at  $-196\text{ }^{\circ}\text{C}$  of SBA-15 and MCF mesoporous silicas were performed for the determination of surface area (multi-point BET method), total pore volume (at  $P/P_0 = 0.99$ ), and pore size distribution (BJH method using adsorption data) of the SBA-15 and MCF silica samples, which were previously outgassed at  $150\text{ }^{\circ}\text{C}$  for 16 h under  $6.6 \times 10^{-9}$  mbar vacuum using an Automatic Volumetric Sorption Analyzer (Autosorb-1MP, Quantachrome, Boynton Beach, FL, USA).

XRD analyses of polymer organoclay nanocomposites took place on films prepared using a hydraulic press with heated platens, in a Brüker D8 Advance diffractometer with CuK $\alpha$  radiation ( $\lambda = 1.5418\text{ \AA}$ ). The scanning parameters concerning  $2\theta$  range, scanning rate, and step time were 1.6–30 degrees, 0.03 degrees per s, and 1 s, respectively. The d-spacing of the clay-containing samples was estimated from the 001 reflection.

Thermogravimetric analysis (TGA) was carried out using a Perkin-Elmer Pyris-Diamond apparatus. Samples of about 4–6 mg were heated from 25 to  $700\text{ }^{\circ}\text{C}$  at a heating rate of  $10\text{ }^{\circ}\text{C min}^{-1}$  in flowing N<sub>2</sub>, with a flow rate of  $30\text{ mL min}^{-1}$ .

The mechanical properties of the obtained PS-composite films were assessed via tensile measurements. Tests were performed according to ASTM D638 using a Simantzu AX-G 5kNt instrument. Three to five samples of each film were clamped between the grips (30 mm initial distance) and tensioned at a crosshead speed of 5 mm/min. The shape of the samples was dumbbell, with gauge dimensions of  $10 \times 3 \times 0.22\text{ mm}$ . Force (N) and deformation (mm) were recorded during the test. Baseline samples (polystyrene films, not containing fillers) were tested at the beginning of each set of samples for comparison.

Oxygen transmission rate (OTR) was measured using an Oxygen Permeation Analyzer (SYSTECH Illinois model 8001) according to Standard Method D 3985-81 (ASTM 1989). Testing was performed at  $23\text{ }^{\circ}\text{C}$  in a dry environment (0% RH). Oxygen transmission rate (OTR) was obtained in cc O<sub>2</sub>/m<sup>2</sup> day. For each OTR value, two samples were tested at least.

## 3. Results

### *Mesoporous Silicas' Characterization*

The SEM images of SBA-15 and MCF mesoporous silicas are presented in Figure 1. As it can be seen (Figure 1a), SBA-15 silica is comprised of small primary particles ( $\sim 0.5\text{ }\mu\text{m}$ ) with well-formed surfaces and edges, which are aggregated to longer, wormlike assemblies of ca. 5–20  $\mu\text{m}$ . The SEM images of MCF (Figure 1b) showed the presence of relatively smaller primary particles ( $\sim 0.2\text{--}0.5\text{ }\mu\text{m}$ ), which are, however, more densely aggregated compared to those of SBA-15 and form larger particles of ca. 5–20  $\mu\text{m}$ .

TEM images shown in Figure 2 verify the well-formed structure of the studied mesoporous silicas. The parallel, tubular mesopores of SBA-15 with the characteristic hexagonal ordering can be seen in Figure 2a and the inset image respectively, while the foam-like structure of the spherical pores of MCF can be seen in Figure 2b.

The porous characteristics of the SBA-15 and MCF mesoporous silicas were studied by N<sub>2</sub> porosimetry at  $-196\text{ }^{\circ}\text{C}$ . In Table 1, the corresponding data (BET-specific surface area, total, micro- and meso/macro-pore volume, and average mesopore size) are tabulated. The adsorption isotherms of both SBA-15 and MCF (not shown for brevity) are of type IV according to the IUPAC classification [27] typical for such type of ordered mesoporous materials. The mesoporous silicas exhibit relatively high specific surface area (BET method)

compared to classical sol-gel silicas or fumed nanosilicas, being 701 and 572 m<sup>2</sup>/g for SBA-15 and MCF, respectively. They also exhibit high total pore volume, with that of MCF being relatively higher, i.e., 1.418 cc/g compared to 1.081 cc/g of SBA-15. Their pore volume is mainly attributed to meso/macropore volume, as the contribution of micropores is minimum. The average mesopore size (diameter) of the mesoporous silicas is also different, with that of SBA-15 being 8.4 nm and of MCF being 18.0 nm. It is well-known that SBA-15 comprises of tubular mesopores in an ordered hexagonal array, while MCF exhibits a cellular pore morphology of relatively larger size pores, giving a foam-like texture [28–30].

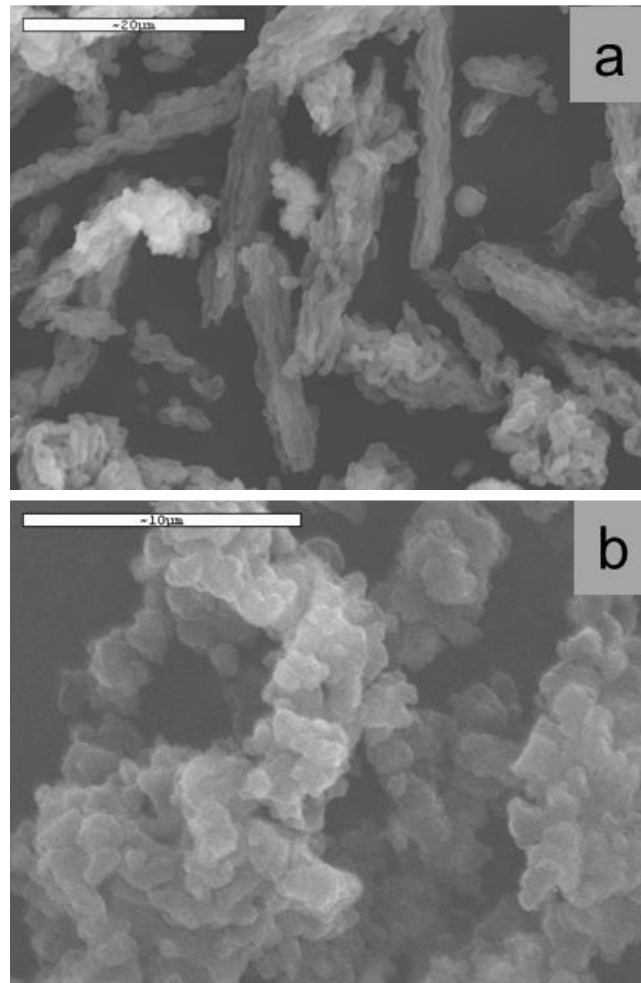


**Figure 1.** SEM images of (a) SBA-15 (size bar: 20 μm) and (b) MCF mesoporous silicas (size bar: 10 μm).

**Table 1.** Porosity data of SBA-15 and MCF mesoporous silicas.

Material	SSA <sup>(1)</sup> (m <sup>2</sup> /g)	Total Pore Volume <sup>(2)</sup> (cc/g)	Average Pore Diameter <sup>(3)</sup> (nm)
SBA-15	701	1.081	8.4
MCF	572	1.418	18.0

<sup>(1)</sup> Multi-point BET method using N<sub>2</sub> adsorption data at −196 °C. <sup>(2)</sup> At P/Po = 0.99. <sup>(3)</sup> Average mesopore pore diameter by BJH analysis using N<sub>2</sub> adsorption data.

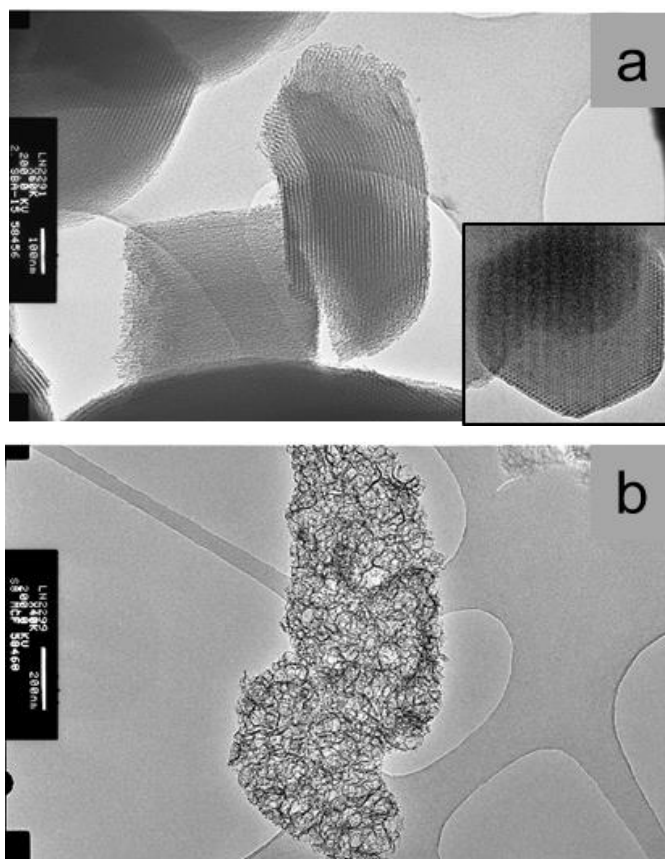


**Figure 2.** TEM images of (a) SBA-15 (size bar: 100 nm) and (b) MCF mesoporous silicas (size bar: 200 nm).

XRD patterns of the prepared PS organoclay nanocomposites are shown in Figure 3. Figure 3a graphs correspond to materials prepared using orgMMT and Figure 3b to materials prepared using orgZenith as nanofiller. The estimated d-spacing from the XRD analysis as well as the temperatures for 50% weight loss ( $T_{50\%}$ ) of TGA of the prepared materials are presented in Table 2. From the XRD patterns (Figure 3a,b) and the corresponding results (Table 2), an increase in d-spacing is shown for the PS-nanocomposites compared to the corresponding organoclays, from 3.04 and 3.28 nm for orgMMT and orgZenith to 3.81 and 4.00 nm for the PS-nanocomposite with 1 wt% orgMMT or orgZenith loading, respectively. This is what one may expect for an intercalated structure where the polymer chains are incorporated between the silicate layers, increasing their gallery height but maintaining their layered stacking with alternating polymer/silicate layers.

In the case of 3 and 5 wt% nanofiller (orgMMT and orgZenith) loadings, a small decrement in the  $d_{001}$ -spacing is observed. This decrement in the  $d_{001}$ -spacing after mixing with the polymeric matrix may be attributed to a decrease in the mobility of the carbon chain of the surfactant with a concomitant reduction from their arrangements in the layers. Also, this shift to lower  $d_{001}$ -spacing is usually attributed to the loss of unbound surfactant from the gallery or to surfactant degradation [31].

Characteristic TGA curves of pristine PS and its composites are shown in Figure 4. TGA results indicate improvement of the thermal stability for PS-nanocomposites with clay nanofillers compared to net polystyrene. For composites prepared with SBA-15 and MCF, only the melt compounding method provided materials with improved thermal stability. The thermal analysis results of polymer composites with SBA-15 and MCF, prepared via the solution casting method, are indicative of conventional composite preparation. Worst thermal resistance in comparison to pristine PS was observed. The improved thermal stability of PS/mesoporous silicas microcomposites prepared via melt mixing may be

attributed to the increased interfacial interactions between the polymeric chains and the high surface area walls of mesoporous silicas. On the other hand, the different thermal behavior between the mesoporous silica composites prepared via the two synthetic routes (solution casting and melt intercalation) could be a result of variable pore impregnation by macromolecular chains. More specifically, the vigorous stirring applied in solution casting prevents the high molecular weight PS chains from entering the silica pores, while under melt mixing, the PS chains have the appropriate mobility to enter the silica pores without hindrance.

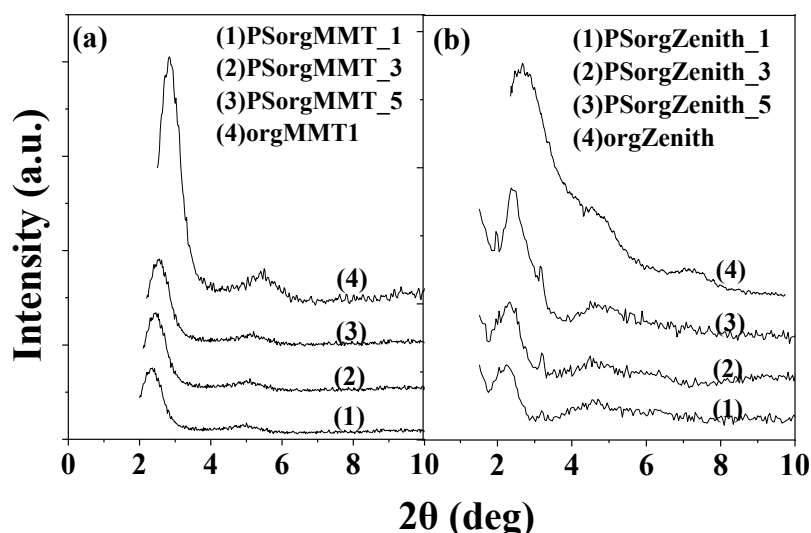


**Figure 3.** XRD patterns of PS-nanocomposites reinforced with (a) orgMMT and (b) orgZenith nanofillers. The corresponding curves for organo-modified nanofillers have been added for comparison.

**Table 2.**  $2\theta$  values of 001 clay reflection, basal spacing ( $d_{001}$ ) of clays in the PS nanocomposites, as well as the average values of the elastic modulus, tensile stress, and elongation at break, temperature for 50% weight loss ( $T_{50\%}$ ), and oxygen transmission rate (for two film thickness) for net polymer and composites.

Materials	$2\theta_{001}$ (°)	$d_{001}$ (nm)	Tensile Stress at Break (MPa)	Elongation at Break (%)	Elastic Modulus (MPa)	$T_{50\%}$ (°C)	OTR (cc/m <sup>2</sup> day) Thickness = 200–300 $\mu$ m	OTR (cc/m <sup>2</sup> day) Thickness = 400–500 $\mu$ m
PS	-	-	71 $\pm$ 0.5	3.1 $\pm$ 0.1	2560 $\pm$ 65	391	1200 $\pm$ 120	520 $\pm$ 50
orgMMT	2.9	3.04						
PSorgMMT_1	2.3	3.81	55 $\pm$ 0.5	2.6 $\pm$ 0.1	2750 $\pm$ 40	403	723 $\pm$ 80	362 $\pm$ 50
PSorgMMT_3	2.4	3.67	59 $\pm$ 0.5	2.4 $\pm$ 0.1	2940 $\pm$ 50	407	628 $\pm$ 90	261 $\pm$ 50
PSorgMMT_5	2.5	3.54	63 $\pm$ 0.5	2.3 $\pm$ 0.1	3120 $\pm$ 45	409	640 $\pm$ 70	238 $\pm$ 50
orgZenith	2.7	3.28						
PSorgZenith_1	2.2	4.00	68 $\pm$ 0.5	3.1 $\pm$ 0.1	2500 $\pm$ 50	423	748 $\pm$ 80	360 $\pm$ 50
PSorgZenith_3	2.3	3.81	66 $\pm$ 0.5	3.5 $\pm$ 0.1	2590 $\pm$ 65	427	611 $\pm$ 80	280 $\pm$ 50
PSorgZenith_5	2.4	3.67	65 $\pm$ 0.5	3.4 $\pm$ 0.1	2610 $\pm$ 70	428	582 $\pm$ 90	262 $\pm$ 50
SBA-15	-	-						
PS_SBA_1	-	-	50 $\pm$ 0.5	2.3 $\pm$ 0.1	2300 $\pm$ 220	355		
PS_SBA_3	-	-	46 $\pm$ 0.5	2.0 $\pm$ 0.1	2200 $\pm$ 280	351		
PS_SBA_5	-	-	41 $\pm$ 0.5	2.4 $\pm$ 0.1	1800 $\pm$ 320	358		
mPS_SBA_1	-	-	98 $\pm$ 0.5	1.1 $\pm$ 0.1	3540 $\pm$ 185	407		140 $\pm$ 30
mPS_SBA_3	-	-	102 $\pm$ 0.5	0.9 $\pm$ 0.1	3740 $\pm$ 190	406		123 $\pm$ 20
mPS_SBA_5	-	-	107 $\pm$ 0.5	0.8 $\pm$ 0.1	3810 $\pm$ 160	406		110 $\pm$ 20
MCF	-	-						
PS_MCF_1	-	-	53 $\pm$ 0.5	2.1 $\pm$ 0.1	2600 $\pm$ 250	323		

Table 2. Cont.

Materials	$2\theta_{001}$ ( $^{\circ}$ )	$d_{001}$ (nm)	Tensile Stress at Break (MPa)	Elongation at Break (%)	Elastic Modulus (MPa)	$T_{50\%}$ ( $^{\circ}$ C)	OTR (cc/m <sup>2</sup> day) Thickness = 200–300 $\mu$ m	OTR (cc/m <sup>2</sup> day) Thickness = 400–500 $\mu$ m
PS_MCF_3	-		39 $\pm$ 0.5	1.7 $\pm$ 0.1	2200 $\pm$ 240	330		
PS_MCF_5	-		32 $\pm$ 0.5	1.5 $\pm$ 0.1	2050 $\pm$ 310	342		
mPS_MCF_1	-		99 $\pm$ 0.5	1.1 $\pm$ 0.1	3630 $\pm$ 180	407		113 $\pm$ 30
mPS_MCF_3	-		104 $\pm$ 0.5	1.0 $\pm$ 0.1	3741 $\pm$ 160	409		96 $\pm$ 20
mPS_MCF_5	-		110 $\pm$ 0.5	0.9 $\pm$ 0.1	3850 $\pm$ 190	411		92 $\pm$ 20

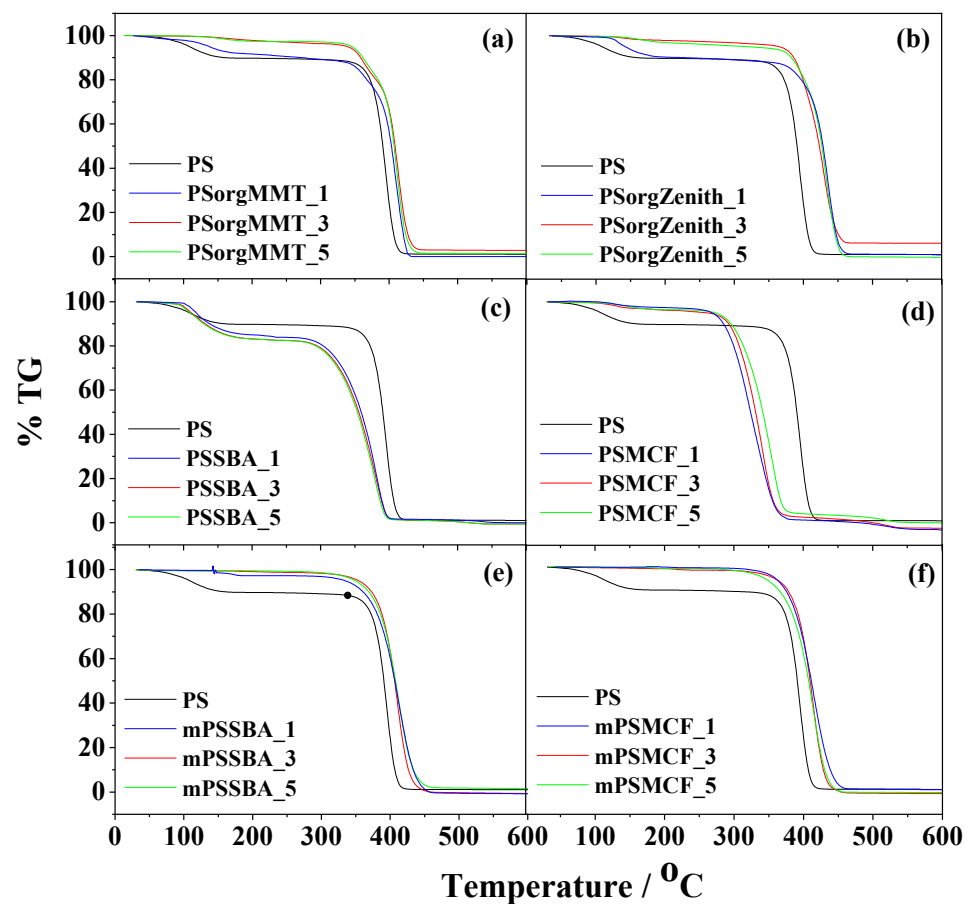


**Figure 4.** TGA curves of all PS-composite reinforced with: (a) orgMMT, (b) orgZenith, (c) SBA-15 (solution casting method), (d) MCF (solution casting method), (e) SBA-15 (melt mixing) and (f) MCF (melt mixing). The corresponding curve for net PS has been added for comparison.

The decomposition temperature,  $T_{50\%}$ , of nanocomposites increased by 12–37  $^{\circ}$ C. This increment is more prevalent for nanocomposites prepared with orgZenith as nanofiller. Especially, PSorgZenith\_5 nanocomposite possesses higher thermal stability in comparison to other PS-nanocomposites obtained by various preparation methods and nanofillers' addition [32]. The thermal stability of polystyrene was also reinforced when OrgMMT or SBA-15 and MCF (only melt compounding method) fillers were added. Increment of  $T_{50\%}$  values up to 20  $^{\circ}$ C was observed.

Regarding the mechanical properties of the tested composites, the average values of elastic modulus (E), as well as tensile strength, and elongation at break values along with those at yield point, are given in Table 2. Typical stress-strain curves for tested polymer composite films are presented in Figure 5. The elastic modulus of the samples

was determined from the slope of the initial elastic region in the stress-strain curves. The yield point is quite significant since it provides information around the formability of the obtained films. The value of  $E$  for the net PS polymer was 2560 MPa and similar values were estimated for the PS-nanocomposites with orgZenith as filler. The addition of orgMMT induces significant reinforcing effects. As the filler's content increased, the  $E$  values were monotonously increased up to 22% in comparison to net PS.

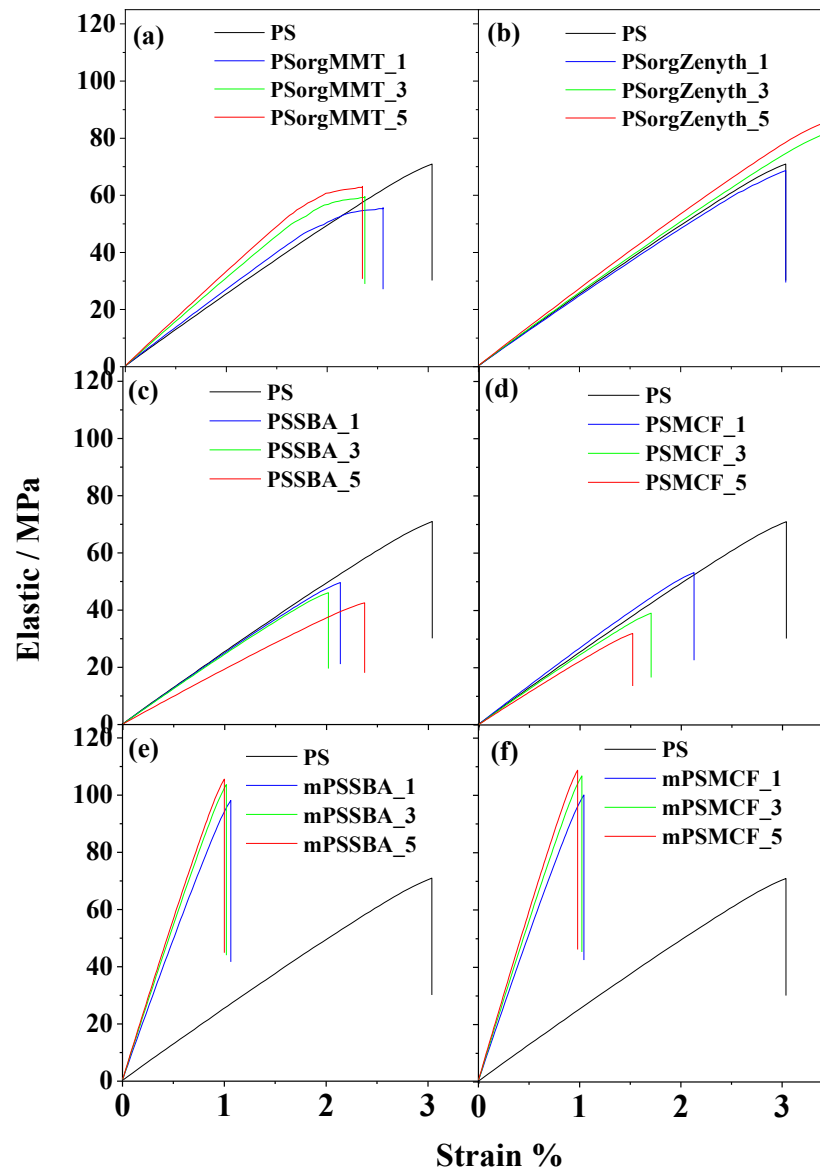


**Figure 5.** Characteristic stress-strain curves of the PS-composites reinforced with: (a) orgMMT, (b) orgZenith, (c) SBA-15 (solution casting method), (d) MCF (solution casting method), (e) SBA-15 (melt mixing) and (f) MCF (melt mixing). The corresponding curve for net PS has been added for comparison.

For composites with SBA-15 and MCF, the  $E$  values exhibit a significant differentiation depending on the preparation method. Particularly, for the microcomposites prepared by the melting process, for both fillers, the value of  $E$  was increased up to 50%, while for the composites received by the solution blending method, the value of  $E$  decreased by 30% when compared with the net PS polymer. The superior mechanical properties induced to the PS microcomposites with silica mesoporous addition (namely SBA-15 and MCF), prepared by melt process, are indicative of good dispersion of particles in the polymer

matrix. Similar to the thermal properties' dependence from the preparation methods of mesoporous silica composites, the improved mechanical properties of microcomposites prepared via the melt process may be attributed to the effective pore impregnation by the polymer chains, leading to increased interfacial interactions between the organic and inorganic phases, while the decreased mechanical properties of composites prepared via solution casting may be attributed to the ineffective pore impregnation.

At the same time, the tensile strength of PS was increased up to 40% after the addition of SBA-15 and MCF, while the addition of organoclays led to negligible differentiation in comparison to net PS. These results confirm the indication referred to above for good particles' dispersion in the polymer matrix for microcomposites received by a melt process. Moreover, the interfacial interactions between the filler and matrix play an important role in the overall mechanical performance of the composite systems. Comparable results about nanoparticle dispersion in polymer matrix were referred [32], where preparation of polystyrene nanocomposites with functionalized carbon nanotubes by melt and solution mixing was studied. Dispersion of MWCNTs, as well as electrical, thermal, and rheological properties of the nanocomposites, were analyzed. Independent of the preparation procedure, the best MWCNT macro-dispersion was achieved when in situ synthesized polystyrene masterbatch (DPS) was applied. When using solution mixing, the difference in macro-dispersion between different MWCNTs is less pronounced in comparison to melt mixing.

Elongation at break was decreased with the increase of the filler's content. This decrement is more prevalent for microcomposites obtained by melt mixing with SBA-15 and MCF. The presence of particles in the polymer matrix has been associated with constrained regions that enhance stiffness and strength, but at the same time result in lowering the elongation properties due to the prevention of easy sliding of polymer chains against each other.

Oxygen transmission rates values (OTR) for two film thicknesses for all obtained films are tabulated in Table 2. Organoclay (orgMMT and orgZenith) addition leads to a decrease in OTR values. OTR was considerably decreased with increasing organoclay loading from 1 to 5 wt% and with increasing the film thickness. This decrement reaches up to 50% for high organoclay content films in comparison to pristine PS film. These results are attributed first of all to the fact that in nanocomposites, gas molecules have to take a long and tortuous way around the impermeable clay layers, which are distributed in the polymer matrix, in comparison with pristine polymer, where the penetration of the film is much easier.

OTR was surprisingly decreased for films obtained with the addition of mesoporous silicas (SBA-15 and MCF) in the polymer matrix. Decrement above 80% was measured for microcomposites with 5 wt% filler content. As far as we know from the results published in the open literature, similar improvement of oxygen barrier properties was observed in the case of polystyrene-clay nanocomposites prepared using 10 wt% of compatibilizer, 2 wt% of clay, and the combination of in situ polymerization and the melt compounding method [33].

There is no comparative study of barrier properties of polymer composites with 2D (i.e., clay, graphene) or 3D fillers published in the open literature. In a previous study [34], the correlation between the aspect ratio of the clay and the barrier properties was conducted, and it was shown that the best barrier properties were obtained in polymer nanocomposites with fully exfoliated clay minerals. Comparing the OTR results for the various fillers used in this study, probably, the diminished OTR values obtained are indicative of well-dispersed mesoporous silicas in the polymer matrix.

#### 4. Conclusions

PS-hybrid composites were prepared using two organo-modified clays and two mesoporous silicas through the solution mixing and melt compounding processes. Intercalated nanocomposite structure was obtained using organoclay as a nanofiller.

TGA results indicated improvement in thermal stability, of PS-nanocomposites, compared to the pristine polymer. This enhancement was more prevalent for nanocomposites prepared with orgZenith organoclay.

Tensile measurements evidenced an increase in elastic modulus of polymer up to 22% with the addition of orgMMT. This increment was more prevalent (up to 50%) for microcomposites prepared by the melting process using mesoporous silicas as fillers.

Organoclay (orgMMT and orgZenith) addition led to a decrease in OTR values. This decrement reached up to 50% for high organoclay content films in comparison to PS film. Decrement above 80% was measured for microcomposites with mesoporous silicas and 5 wt% filler content.

The superior mechanical properties and the surprising decrement of oxygen permeation induced to the PS microcomposites with mesoporous silicas addition (namely SBA-15 and MCF), prepared by the melt process, are indicative of excellent dispersion of inorganic particles in the polymer matrix.

**Author Contributions:** Conceptualization, A.L., D.G., M.A.K. and K.S.T.; methodology, A.L., A.E.G. and K.S.T.; validation, A.L. and A.E.G.; investigation, A.E.G., P.X., D.J.G. and M.B.; resources, A.L., D.G., M.A.K. and K.S.T.; Writing—original draft preparation, A.L., A.E.G. and D.J.G.; Writing—review and editing, A.L., D.G., M.A.K. and K.S.T.; visualization, A.L., A.E.G. and D.J.G.; supervision, A.L. All authors have read and agreed to the published version of the manuscript.

**Funding:** This research received no external funding.

**Conflicts of Interest:** The authors declare no conflict of interest.

## References

- Loeffen, A.; Cree, D.E.; Sabzevari, M.; Wilson, L.D. Effect of Graphene Oxide as a Reinforcement in a Bio-Epoxy Composite. *J. Compos. Sci.* **2021**, *5*, 91. [CrossRef]
- Blanco, I. The Rediscovery of POSS: A Molecule Rather than a Filler. *Polymers* **2018**, *10*, 904. [CrossRef]
- Ali Charfi, M.; Mathieu, R.; Chatelain, J.-F.; Ouellet-Plamondon, C.; Lebrun, G. Effect of Graphene Additive on Flexural and Interlaminar Shear Strength Properties of Carbon Fiber-Reinforced Polymer Composite. *J. Compos. Sci.* **2020**, *4*, 162. [CrossRef]
- Arrigo, R.; Teresi, R.; Gambarotti, C.; Parisi, F.; Lazzara, G.; Dintcheva, N.T. Sonication-Induced Modification of Carbon Nanotubes: Effect on the Rheological and Thermo-Oxidative Behaviour of Polymer-Based Nanocomposites. *Materials* **2018**, *11*, 383. [CrossRef] [PubMed]
- Cicala, G.; Tosto, C.; Latteri, A.; La Rosa, A.D.; Blanco, I.; Elsabbagh, A.; Russo, P.; Ziegmann, G. Green Composites Based on Blends of Polypropylene with Liquid Wood Reinforced with Hemp Fibers: Thermomechanical Properties and the Effect of Recycling Cycles. *Materials* **2017**, *10*, 998. [CrossRef] [PubMed]
- Lazzara, G.; Cavallaro, G.; Panchal, A.; Fakhrullin, R.; Stavitskaya, A.; Vinokurov, V.; Lvov, Y. An Assembly of Organic-Inorganic Composites Using Halloysite Clay Nanotubes. *Curr. Opin. Colloid Interface Sci.* **2018**, *35*, 42–50. [CrossRef]
- Mohan, V.B.; Lau, K.; Hui, D.; Bhattacharyya, D. Graphene-Based Materials and Their Composites: A Review on Production, Applications and Product Limitations. *Compos. Part B Eng.* **2018**, *142*, 200–220. [CrossRef]
- Blanco, I.; Bottino, F.A.; Cicala, G.; Cozzo, G.; Latteri, A.; Recca, A. Synthesis and Thermal Characterization of New Dumbbell Shaped POSS/PS Nanocomposites: Influence of the Symmetrical Structure of the Nanoparticles on the Dispersion/Aggregation in the Polymer Matrix. *Polym. Compos.* **2015**, *36*, 1394–1400. [CrossRef]
- Bajwa, D.S.; Shojaeiarani, J.; Liaw, J.D.; Bajwa, S.G. Role of Hybrid Nano-Zinc Oxide and Cellulose Nanocrystals on the Mechanical, Thermal, and Flammability Properties of Poly (Lactic Acid) Polymer. *J. Compos. Sci.* **2021**, *5*, 43. [CrossRef]
- Albiter, E.; Merlano, A.S.; Rojas, E.; Barrera-Andrade, J.M.; Salazar, Á.; Valenzuela, M.A. Synthesis, Characterization, and Photocatalytic Performance of ZnO–Graphene Nanocomposites: A Review. *J. Compos. Sci.* **2021**, *5*, 4. [CrossRef]
- Alexandre, M.; Dubois, P. Polymer-Layered Silicate Nanocomposites: Preparation, Properties and Uses of a New Class of Materials. *Mater. Sci. Eng. R Rep.* **2000**, *28*, 1–63. [CrossRef]
- Giannelis, E.P. Polymer Layered Silicate Nanocomposites. *Adv. Mater.* **1996**, *8*, 29–35. [CrossRef]
- Giannakas, A.; Spanos, C.G.; Kourkoumelis, N.; Vaimakis, T.; Ladavos, A. Preparation, Characterization and Water Barrier Properties of PS/Organo-Montmorillonite Nanocomposites. *Eur. Polym. J.* **2008**, *44*, 3915–3921. [CrossRef]
- Giannakas, A.; Xidas, P.; Triantafyllidis, K.S.; Katsoulidis, A.; Ladavos, A. Preparation and Characterization of Polymer/Organosilicate Nanocomposites Based on Unmodified LDPE. *J. Appl. Polym. Sci.* **2009**, *114*, 83–89. [CrossRef]
- Panwar, A.; Choudhary, V.; Sharma, D.k. Review: A Review: Polystyrene/Clay Nanocomposites. *J. Reinf. Plast. Compos.* **2011**, *30*, 446–459. [CrossRef]
- Di Pasquale, G.; Pollicino, A. Properties of Polystyrene Clay Nanocomposites Prepared Using Two New Imidazolium Surfactants. Available online: <https://www.hindawi.com/journals/jnm/2017/2594958/> (accessed on 20 November 2019).

17. Pugazhenth, G.; Suresh, K.; Vinoth Kumar, R.; Kumar, M.; Rajkumar Surin, R. A Simple Sonication Assisted Solvent Blending Route for Fabrication of Exfoliated Polystyrene (PS)/Clay Nanocomposites: Role of Various Clay Modifiers. *Mater. Today Proc.* **2018**, *5*, 13191–13210. [CrossRef]
18. Dağ, S.E.; Bozkurt, P.A.; Eroğlu, F.; Çelik, M. Preparation, Characterization, and Properties of Polystyrene/Na-Montmorillonite Composites. *J. Thermoplast. Compos. Mater.* **2019**, *32*, 1078–1091. [CrossRef]
19. Kourki, H.; Famili, M.H.N.; Mortezaei, M.; Malekipirbazari, M. Mixing Challenges for SiO<sub>2</sub>/Polystyrene Nanocomposites. *J. Thermoplast. Compos. Mater.* **2018**, *31*, 709–726. [CrossRef]
20. Jeon, I.-Y.; Baek, J.-B. Nanocomposites Derived from Polymers and Inorganic Nanoparticles. *Materials* **2010**, *3*, 3654–3674. [CrossRef]
21. Kango, S.; Kalia, S.; Celli, A.; Njuguna, J.; Habibi, Y.; Kumar, R. Surface Modification of Inorganic Nanoparticles for Development of Organic–Inorganic Nanocomposites—A Review. *Prog. Polym. Sci.* **2013**, *38*, 1232–1261. [CrossRef]
22. Khezri, K.; Roghani-Mamaqani, H. Effect of MCM-41 Nanoparticles on ARGET ATRP of Styrene: Investigating Thermal Properties. Available online: <https://journals.sagepub.com/doi/abs/10.1177/0021998314535961?journalCode=jema> (accessed on 20 November 2019).
23. Suresh, K.; Kumar, R.V.; Pugazhenth, G. Processing and Characterization of Polystyrene Nanocomposites Based on CoAl Layered Double Hydroxide. *J. Sci. Adv. Mater. Devices* **2016**, *1*, 351–361. [CrossRef]
24. Meynen, V.; Cool, P.; Vansant, E.F. Verified Syntheses of Mesoporous Materials. *Microporous Mesoporous Mater.* **2009**, *125*, 170–223. [CrossRef]
25. Karakoulia, S.A.; Triantafyllidis, K.S.; Lemonidou, A.A. Preparation and Characterization of Vanadia Catalysts Supported on Non-Porous, Microporous and Mesoporous Silicates for Oxidative Dehydrogenation of Propane (ODP). *Microporous Mesoporous Mater.* **2008**, *110*, 157–166. [CrossRef]
26. Achilias, D.S.; Gerakis, K.; Giliopoulos, D.J.; Triantafyllidis, K.S.; Bikiaris, D.N. Effect of High Surface Area Mesoporous Silica Fillers (MCF and SBA-15) on Solid State Polymerization of PET. *Eur. Polym. J.* **2016**, *81*, 347–364. [CrossRef]
27. Robens, E. Adsorption by Powders and Porous Solids. F. Rouquerol, J. Rouquerol, K. Sing, Academic Press, San Diego 1999, ISBN: 0-12-598920-2, 467 S. £79.95. *Vak. Forsch. Und Prax.* **1999**, *11*, 191. [CrossRef]
28. Zhao, D.; Huo, Q.; Feng, J.; Chmelka, B.F.; Stucky, G.D. Nonionic Triblock and Star Diblock Copolymer and Oligomeric Surfactant Syntheses of Highly Ordered, Hydrothermally Stable, Mesoporous Silica Structures. *J. Am. Chem. Soc.* **1998**, *120*, 6024–6036. [CrossRef]
29. Schmidt-Winkel, P.; Lukens, W.W.; Zhao, D.; Yang, P.; Chmelka, B.F.; Stucky, G.D. Mesocellular Siliceous Foams with Uniformly Sized Cells and Windows. *J. Am. Chem. Soc.* **1999**, *121*, 254–255. [CrossRef]
30. Li, L.; Li, B.; Hood, M.A.; Li, C.Y. Carbon Nanotube Induced Polymer Crystallization: The Formation of Nanohybrid Shish–Kebabs. *Polymer* **2009**, *50*, 953–965. [CrossRef]
31. Paul, D.R.; Robeson, L.M. Polymer Nanotechnology: Nanocomposites. *Polymer* **2008**, *49*, 3187–3204. [CrossRef]
32. Faraguna, F.; Pötschke, P.; Piontecka, J. Preparation of polystyrene nanocomposites with functionalized carbon nanotubes by melt and solution mixing: Investigation of dispersion, melt rheology, electrical and thermal properties. *Polymer* **2017**, *132*, 325–341. [CrossRef]
33. Panwar, A.; Choudhary, V.; Sharma, D. Role of Compatibilizer and Processing Method on the Mechanical, Thermal and Barrier Properties of Polystyrene/Organoclay Nanocomposites. Available online: <https://journals.sagepub.com/doi/abs/10.1177/0731684413477770> (accessed on 20 November 2019).
34. Yano, K.; Usuki, A.; Okada, A. Synthesis and Properties of Polyimide-Clay Hybrid Films. *J. Polym. Sci. Part A Polym. Chem.* **1997**, *35*, 2289–2294. [CrossRef]